Published online 6 February 2018

Nucleic Acids Research, 2018, Vol. 46, No. 8 ***e48***
doi: 10.1093/nar/gky062

A small, portable RNA device for the control of exon skipping in mammalian cells

Marc Vogel[1], Julia E. Weigand[1], Britta Kluge[1], Manuel Grez[2] and Beatrix Suess[1,*]

[1]Department of Biology, Technical University Darmstadt, Schnittspahnstr. 10, 64287 Darmstadt, Germany and [2]Institute for Tumor Biology and Experimental Therapy, Georg-Speyer-Haus, Paul-Ehrlich-Str. 42–44, 60596 Frankfurt/M, Germany

Received September 11, 2016; Revised January 15, 2018; Editorial Decision January 20, 2018; Accepted January 29, 2018

ABSTRACT

Splicing is an essential and highly regulated process in mammalian cells. We developed a synthetic riboswitch that efficiently controls alternative splicing of a cassette exon in response to the small molecule ligand tetracycline. The riboswitch was designed to control the accessibility of the 3′ splice site by placing the latter inside the closing stem of a conformationally controlled tetracycline aptamer. In the presence of tetracycline, the cassette exon is skipped, whereas it is included in the ligand's absence. The design allows for an easy, context-independent integration of the regulatory device into any gene of interest. Portability of the device was shown through its functionality in four different systems: a synthetic minigene, a reporter gene and two endogenous genes. Furthermore, riboswitch functionality to control cellular signaling cascades was demonstrated by using it to specifically induce cell death through the conditionally controlled expression of CD20, which is a target in cancer therapy.

INTRODUCTION

Synthetic biology has provided innovative solutions for challenges in fields ranging from control of the flow of genetic information, material production, bioremediation or diagnostics up to therapeutic applications in medicine through the design of new biological components. The development of genetic elements capable of regulating gene expression in response to internal or external stimuli thus forms the basis of many of these applications (1). Regulatory RNA molecules have the distinct advantage that they can operate in a protein-independent manner, which allows (i) fast regulatory responses, (ii) genetic modularity and portability, and (iii) a flexible and modular combination of different platforms to achieve a broad spectrum of regulatory outputs. This makes RNA an attractive molecular scaffold for designing genetic control elements (2). The value of RNA molecules is further enhanced by the addition of riboswitches, i.e. small structured RNA elements that regulate gene expression in response to a small molecule ligand. Their use allows for spatial, temporal and dosage control of gene expression. They couple the binding of a small molecule ligand to the so-called 'aptamer domain' with a conformational change in the downstream 'expression platform', which then determines the system output (3). The modular organization of riboswitches and the possibility to identify RNA aptamer domains *de novo* using an *in vitro* selection process (SELEX, (4,5)) stimulated the development of synthetic riboswitches as artificial genetic control devices in biotechnology and synthetic biology over the past decade (6). However, whereas riboswitch functionality, robustness and reliability have successfully been established in many bacterial model organisms and yeast, less effort has gone into transferring synthetic riboswitches into mammalian cell culture, transgenic animals or plants (7).

RNA aptamers are the centerpiece of constructing synthetic riboswitches (8,9). They bind their cognate ligand with high affinity and specificity, and therefore, they represent perfect sensing domains. Unfortunately, despite the fact that several dozen small molecule binding aptamers have been selected in the last years, only a handful of them turned out to be appropriate for the construction of regulatory devices (7). The tetracycline (tc)-binding aptamer (Figure 1A) was revealed as an excellent building block for the development of synthetic riboswitches (10). It binds its ligand tc with a dissociation constant of 600 pM and can distinguish between tc and doxycycline, a closely related analogue that differs only by the position of one hydroxyl group (11). Moreover, tc is a well-characterized therapeutic agent of low toxicity and enters nearly all cells, including passage of the blood-brain barrier and placenta. The structural stabilization of the tc aptamer upon ligand binding has been used to regulate gene expression in different ways, either as a simple 'road block' to regulate translation initiation in yeast or by the sequestration of protein binding sites to inhibit translation initiation in

*To whom correspondence should be addressed. Tel: +49 6151 1622000; Fax: +49 6151 1622003; Email: bsuess@bio.tu-darmstadt.de

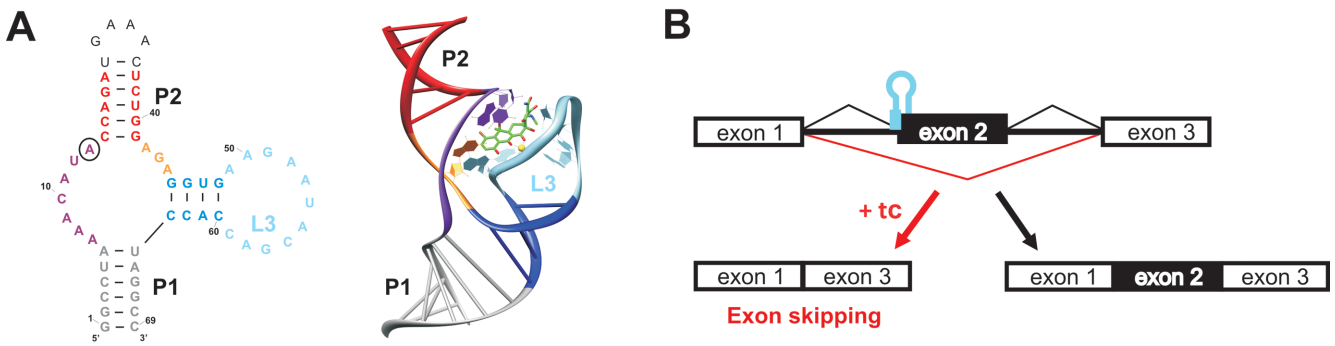

Figure 1. Implementation of the tc aptamer for the regulation of exon skipping. (**A**) Shown is the secondary (left) and the tertiary (right) structure of the tc aptamer. The crystal structure was solved in the ligand-bound state (59). Corresponding stems (P) or loops (L) are colored in the secondary and tertiary structures. Tc is shown in green with the associated magnesium ion in yellow. Tc-contacting bases are displayed in the tertiary structure. Position A13 is circled. (**B**) Scheme of the splicing device. Exons are displayed as boxes and introns as lines. To control splicing, the 3′ SS (indicated in blue) was included in the closing stem P1 of the tc aptamer, which led to skipping exon 2 in the presence of tc.

archaea or intron retention in yeast (12–15). Additionally, the aptamer has successfully been used for the construction of synthetic riboswitches with changed ligand binding specificity (16) or as sensing domain for the construction of allosterically controlled ribozymes both in yeast and mammalian cells (17–19).

In this study, we attempted to control alternative splicing in mammalian cells. Alternative splicing is the major source of our proteome's diversity. More than 90% of all human genes are alternatively spliced, and missplicing is often associated with severe diseases (20,21). The most predominant mechanism of alternative splicing is exon skipping (21). Programmed changes in alternative splicing offer an additional layer of controlling gene expression. In consequence, control of alternative splicing offers an alternative and novel approach for the design of synthetic riboswitches in higher eukaryotes, a group for which most attempts to develop such regulators have been unsuccessful to date. (6). Consequently, by modulating the accessibility of essential splicing elements, such as the 5′ splice site (SS), the branch point or the 3′ SS, engineered riboswitches can be developed to control both constitutive and alternative splicing.

Preliminary work with a basic proof-of-principle approach placed a theophylline aptamer close to the 3′ SS, and as a result observed a 4-fold reduction in splicing efficiency upon addition of theophylline using an *in vitro* splicing assay. These data indicate that theophylline binding to the aptamer specifically blocks recognition of the 3′ SS (22). The aptamer was also used to modulate splicing efficiency of a minigene construct in HeLa cells by controlling the branch site accessibility. RT-PCR data indicate a 2-fold reduced exon skipping in the absence of 1 mM theophylline (23). The data suggest that the control of alternative splicing by small molecule binding aptamers is feasible. However, no further experiments were performed demonstrating control of protein output or genetic modularity. There are alternative strategies to control splicing that make use of protein-controlled RNA devices. For instance, the RNA binding properties of signaling proteins like NFkB or β-catenine have been exploited. The respective RNA recognition motifs have been cloned into a small exon. Binding of the respective proteins to the modified exon reduced its splicing up to 4-fold and allowed efficient control of Wnt signaling (24). An alternative protein-responsive device makes use of a similar mechanism developed for application in plants (25). In this example, a suicide exon was developed which can be inserted into the open reading frame of any gene of interest inhibiting gene expression by premature termination. The expression of the transgenes can then be activated by exon skipping in response to the binding of the L4 protein to the suicide exon. Examples of natural riboswitches outside the bacterial kingdom (plant, filamentous fungi) are rare and to date have been found to exclusively regulate gene expression through alternative splicing (26–29). When tested in the context of reporter constructs, however, gene regulation of these riboswitches was only modest (30). In sum, despite the extraordinary importance of alternative splicing for gene regulation, the number of synthetic splicing devices is rather small and suggests that the full potential for their development has been far from realized to date.

In this study, we exploited the tc aptamer to develop a synthetic RNA device for the conditional control of exon skipping in mammalian cells. We developed an exon whose splicing can be controlled by direct binding of tc to the aptamer sequence, thereby controlling accessibility of the 3′ SS without the need of any further protein cofactors. This exon can be inserted into any gene of interest with the result of gene expression control when 50 μM tc is added. We confirmed the genetic modularity of the splicing device by demonstrating its functionality in four different genes and its independence on the cell type and promoter used. The combination with a tc-controlled ribozyme could maximize the regulatory output. Finally, we applied the splicing device for efficient control of cell survival through tc-controlled expression of the CD20 surface receptor. Such a potent kill switch can now be used as safety device for gene therapeutic applications and impressively demonstrates the potential of our newly developed splicing control element.

MATERIALS AND METHODS

Plasmid construction

Minigene. A chimeric three-exon minigene named pMA-i0 was used (31). Exons 1 and 3 and both introns were derived from the Chinese hamster dihydrofolate reductase gene. Exon 2 is completely synthetic and does not contain any enhancer or silencer sequences. The minigene is controlled by a CMV promoter and is terminated by an SV40 polyA site (Supplementary Figure S1). The tc aptamer was cloned into the minigene by overlap extension PCR and standard restriction ligation using the unique restriction sites for NotI and NheI.

Luciferase constructs. The vectors pWHE200 and pWHE237 were used for luciferase reporter gene assays (kindly provided by C. Berens, unpublished data). Both vectors carry the *luc*+ gene driven by different promoters. pWHE200 contains the SV40 promoter and pWHE237 the CMV promoter. Intron 2 of the human β-globin gene (*bgl2* intron) was inserted into the *luc*+ gene (30 nt downstream of the start codon using the sequence 5′-GTGAGT//CCACAG-3′ as an intron boundary). Exon 2 of the minigene constructs M1-M5 flanked by 150 nt of intronic sequences up- and downstream was cloned into the middle of the *bgl2* intron (flanking sequence 5′-TTATACAT//ATTTTATGG-3′) by overlap extension PCR and standard restriction ligation, which resulted in the vectors pWHE200mod-L2 and pWHE237mod-L1 to -L5 (Supplementary Figure S2). pWHE237mod-L2 was modified by site-directed mutagenesis to change the A at position 13 of the tc aptamer to a U, which resulted in the plasmid pWHE237mod-L2A13U. For the hammerhead constructs, the aptazyme K19 (18) was cloned 16 nt downstream of the stop codon flanked three times by 5′-CAAA-3′ in the vector pWHE237mod-L2 using overlap extension PCR. This cloning resulted in the vector pWHE237mod-L2-K19.

MAX constructs. The vector pFLAG-WT encoding the open reading frame of the *MAX* gene was used for cloning the aptamer-containing constructs MAX1-MAX5 and MAX2-A13U (32). The complete *bgl2* intron containing the tc aptamer-controlled exon 2 from luciferase constructs L1 to L5 and L2-A13U was placed at the natural exon-exon junction between exons 3 and 4 by overlap extension PCR and standard ligation using the unique restriction sites HindIII and ClaI. As a control, the *bgl2* intron containing only exon 2 without tc aptamer was also inserted.

CD20 constructs. The vector pcDNA5/FRT (Invitrogen) was used for chromosomal integration via the Flp-In system. The codon optimized CD20 coding sequence (33) was integrated into pcDNA5/FRT using the restriction sites for NheI and SacI resulting in the construct pFRT/CD20. Afterward, the *bgl2* intron containing the tc aptamer-controlled exon 2 was cloned from the luciferase construct L2 into the CD20 open reading frame (46 bp downstream of the start codon) using the flanking regions 5′-CGCCGAGC//ATTTATGG-3′. This insertion resulted in the vector pFRT/CD20-C2. Cloning was done via overlap extension PCR. All constructs were integrated into the cell line HF1–3 via the Flp-In system (18).

All primer and vector sequences can be provided upon request.

Cell culture and cultivation. HEK293 (ACC 305), MCF-7 (ACC 115) and HeLa (ACC 57) cells used in this study were purchased from the German Collection of Microorganisms and Cell Cultures (DSMZ, Braunschweig, Germany). A-549 cells were purchased from (ATCC Manassas, USA). Cells were grown in T75 flasks using Dulbecco's Modified Eagle's Medium (DMEM, Sigma-Aldrich) supplemented with 10% (v/v) fetal calf serum (Biochrom), 1 mM sodium pyruvate (Gibco), 100 U/ml penicillin (Gibco), and 100 μg/ml streptomycin (Gibco) at 37°C and 5% CO_2. For MCF-7 cells RPMI 1640 (Sigma-Aldrich) was used instead of DMEM. The cells were passaged every 3–4 days, and no cells older than passage 25 were used. HeLa-derived HF1–3 cells (34) were grown using the same conditions with 150 μg/ml zeocin (Invivogen). HeLa HF1–3 cells with stably integrated constructs were grown with 200 μg/ml of hygromycin (Invitrogen).

Stable integration into HeLa HF1-3 cells using the Flp-In system. HeLa HF1–3 cells were transfected with the plasmids pcDNA5/FRT (containing the respective CD20 variant) and pOG44 (recombinase expression plasmid, Invitrogen) at a molar ratio of 1:9 using Lipofectamine® 2000 (Life Technologies) according to the manufacturer's instructions (18,34). The medium was changed 24 h after transfection to DMEM. The cells were selected for stable integration by adding hygromycin (final concentration 200 μg/ml, Invitrogen). After two weeks of incubation with hygromycin, single cells were isolated and analyzed for stable integration by genomic PCR and western blot analysis.

Luciferase reporter assay. A total of 50 000 HeLa, 100 000 MCF-7, 240 000 A-459 or 120 000 HEK293 cells per well were seeded into a 24-well plate. The cells were transfected with 100 ng pWHE200mod or pWHE237mod (expressing the *luc*+ gene) and 100 ng of the plasmid pRL-SV40 (Promega, expressing the *Rluc* gene) in 24-well plates using 1 μl Lipofectamine® 2000 (Life Technologies) per well according to the manufacturer's instructions. The medium was changed 2 h after transfection to DMEM (without phenol red) with or without 50 μM tc. For MCF-7 cells the same amount of RPMI 1640 was used instead of DMEM. The luciferase activity was measured after 24 h using the Dual-Glo® (Promega) system. Luminescence values were recorded using the microplate reader Infinite® M200 (Tecan). For each well, the ratio between the firefly and *Renilla* values was calculated. Each luciferase experiment was performed in triplicate and repeated at least three times.

Western blotting. For the detection of CD20 by western blot analysis, 50,000 HeLa HF1–3 cells per well were seeded into a 12-well plate. The cells were incubated with or without 50 μM tc for 2 days. To detect the MAX protein, 240 000 HEK293 cells were seeded into a 12-well plate and incubated at 37°C and 5% CO_2 for 24

h. The cells were transiently transfected with 400 ng of the pFLAG-MAX variants using 2 μl of Lipofectamine® 2000 (Life Technologies) per well according to the manufacturer's instructions. The medium was changed 2 h after transfection to DMEM with or without 50 μM tc, and the cells were incubated at 37°C and 5% CO_2 for 24 h. The cells were lysed by incubating them with lysis buffer (137 mM NaCl, 10% (v/v) glycerol, 20 mM Tris–HCl, pH 8.0, 2 mM EDTA pH 8.0, 1% (v/v) Igepal and 5 μl protease inhibitor cocktail (Sigma)) for 20 min at 4°C. Cell debris was removed by centrifugation (15 min, 17 000×g, 4°C), and the protein concentration was measured by the Bradford method (Bio-Rad) according to the instructions provided by the manufacturer. Then, 10 μg of protein was separated by SDS-PAGE in an Any kD gel (Bio-Rad) and transferred to a polyvinylidene difluoride membrane using the Trans-Blot® Turbo system (Bio-Rad). Primary antibodies that detect CD20 (ThermoFisher, PA5–16701, 1:500), Hsp60 (Abcam, ab6530, 1:2000) or FLAG (Sigma-Aldrich, A8592–1MG, 1:5 000) and an anti-rabbit horseradish peroxidase-conjugated IgG secondary antibody (Jackson Immunoresearch, 111-035-003, 1:7 000) were used. The ECL reaction was started using the Clarity Western Blotting Substrate (Bio-Rad). The signal was detected using a ChemiDoc Imaging System (Bio-Rad). Each western blot was repeated in two to three independent experiments.

The signal intensity of the MAX western blots was quantified by using the software Image Lab (Bio-Rad). Three independent experiments were performed and the obtained values were normalised the sample MAX-A13U without tc.

RT-PCR analysis. A total of 240 000 HEK293 cells per well were seeded into a 12-well plate. The cells were transfected with 100 ng of plasmid DNA using 2 μl of Lipofectamine® 2000 (Life Technologies) per well according to the manufacturer's instructions. Then, 2 h after transfection, the medium was changed to DMEM with or without 50 μM tc, and the cells were incubated at 37°C and 5% CO_2 for 24 h. RNA was isolated using TRIzol® (Life Technologies). Contaminating DNA was removed with the TURBO DNA-free kit (Life Technologies), and the RNA was quality checked on a 1% (w/v) agarose gel. Next, 1 μg RNA was reverse-transcribed by MuLV (Applied Biosystems) using random hexamers (Fermentas) with the supplied buffers (10 min at 20°C, 15 min at 42°C, 5 min at 99°C). Then, 50 ng cDNA was PCR amplified using Taq polymerase (New England Biolabs, initial denaturation 2 min 96°C, 30 s 96°C, 30 s 54°C, 30 s 72°C, 35 cycles) and analyzed on a 3% (w/v) agarose gel. The amplified products were cloned and sequenced for verification. Each RT-PCR was repeated in two independent experiments. Primers used in this study are listed in Supplementary Table S1.

RT-qPCR analysis. For RT-qPCR analysis the Fast SYBR Green Master Mix (Applied Biosystems) was used and the samples were analyzed on a StepOnePlus Real-Time PCR machine (Applied Biosystems). Primers are listed in Supplementary Table S1. Analysis was performed with samples from three independent experiments in two technical replicates.

AlamarBlue® viability assay. Cell viability was analyzed using the AlamarBlue® cell viability reagent (ThermoFisher). Two thousand cells from the HeLa HF1–3, HF1–3 C2 and HF1–3 CD20 cell lines were seeded into a 96-well plate for the AlamarBlue® assays. Rituximab was added to a final concentration of 10 μg/ml, and 15% (v/v) rabbit serum (Sigma-Aldrich, R4505) was added as a source of complement (33,35). The cells were treated with or without 50 μM tc/doxycycline for 3 days and washed with PBS (PAA). Afterwards, 100 μl DMEM (without phenol red) containing 10% (v/v) AlamarBlue® (Life Technologies) was added. The cells were incubated for 3 h (37°C, 5% CO_2), and the fluorescence of the dye was measured according to the manufacturer's instructions using the microplate reader Infinite® M200 (Tecan). The values were normalized to the corresponding values of untreated cells for each cell line. The assay was repeated in three independent experiments.

To determine the toxicity of tc, 20 000 HEK293 cells per well were seeded into a 96-well plate. The cells were transfected with 20 ng of the plasmids pRL-SV40 and pWHE236mod-L2 using 0.2 μl of Lipofectamine® 2000 (Life Technologies) per well according to the manufacturer's instructions. After 2 h, the medium was changed to DMEM (without phenol red) containing different tc concentrations (0–500 μM). The cells were incubated at 37°C and 5% CO_2 for 24 h. Cell viability was determined as described above using AlamarBlue®.

RESULTS

Tc riboswitch controlled exon skipping within a minigene

The tc aptamer (Figure 1A) was used to construct a regulatory device that can influence whether an exon is included or skipped. For this purpose, the 3′ SS of an intron was included in the aptamer sequence in a way that its recognition became dependent on ligand binding to the aptamer. In the absence of the ligand, the 3′ SS will be recognized and the exon is retained. In contrast, the 3′ SS is sequestered through ligand binding to the aptamer (Figure 1B). A three-exon minigene was used to establish the system with a middle exon 2 that was described to be free of splicing enhancers or silencers (31). The tc aptamer was inserted close to the 5′ end of exon 2 in a way that the 3′ SS of intron 1 was integrated into the closing stem P1 of the aptamer (Figure 2). Breathing of the closing stem has been proposed for the free form of the aptamer (13). Consequently, the 3′ SS was recognized and exon 2 was retained. Ligand binding stiffened P1, which led to a sequestration of the 3′ SS and exon skipping. This flexibility of the closing stem P1 was already exploited to sequester the ribosomal binding site in archaea or to control of intron retention in yeast (13,15).

A set of different constructs were designed which differ in the stability of the aptamer, mainly of the closing stem P1 (GC content, length, ΔG) and of the relative location of the 3′ SS within P1. All constructs are displayed in Figure 2 and Supplementary Figure S3A, and P1 characteristics (stem

length, ΔG) are given in Supplementary Table S2. HEK293 cells were transiently transfected with these constructs and incubated with or without 50 μM tc for 24 h. The splicing pattern was determined by RT-PCR analysis using oligonucleotides binding to exons 1 and 3 (Figure 2B and Supplementary Figure S3B). All constructs except M1 show exon skipping, however to a different degree. For all these constructs, changes in the degree of exon skipping can be seen that are dependent on the presence of the ligand tc. Figure 2 summarizes tc-dependent splicing changes for constructs with increasing stability of stem P1. The constructs M2 and M3 lead to visible exon skipping only in the presence of the ligand. M4 showed slight exon skipping already in the absence of the ligand, whereas exon skipping significantly increased in the presence of tc. In constructs M5 and M6, which harbor five and six additional G-C base pairs, respectively, exon 2 was skipped in the majority of cases in the absence of tc. Consequently, further induction of exon skipping was only marginal upon tc addition. Further stabilization of P1 seemed to prevent exon skipping (M9–M11), and the stabilization of the aptamer via P2 showed only a marginal effect (compare M12 and M8 with M1). A control construct without an aptamer showed the same exon skipping levels in the absence and presence of tc, which showed that splicing was not affected by the ligand.

In sum, these experiments demonstrate that the extent of alternative splicing can be influenced by the tc aptamer with the stability of the P1 stem modulating the dynamic range of exon skipping.

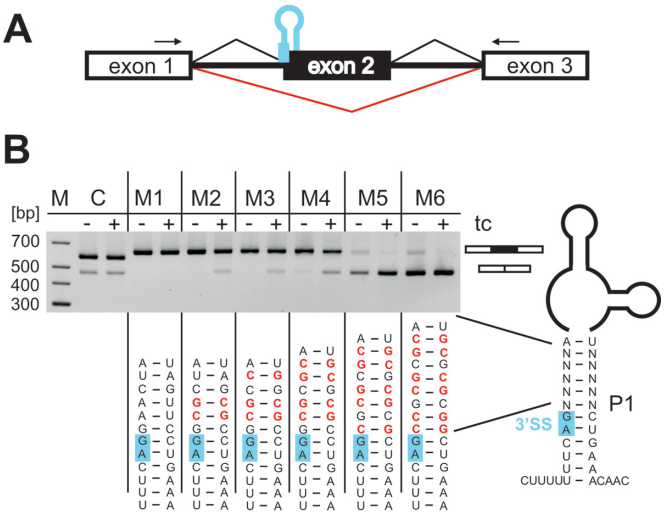

Figure 2. RT-PCR of the minigene constructs. (**A**) Scheme of the splicing device. (**B**) Six different constructs (M1 to M6) were tested in a minigene system (31). HEK293 cells were transiently transfected with the constructs M1-M6 and treated with or without 50 μM tc for 24 h. Total RNA was prepared and used for RT-PCR using primer pairs binding to exons 1 and 3 (indicted by arrows in A). C: control construct without tc aptamer, M: Marker. Constructs M1 to M6 differ in the stability of the closing stem P1. The 3′ SS is marked in blue. Changes in P1 compared to the construct M1 are highlighted in red.

The tc aptamer controlled exon skipping of transgenes

In the next step, tc-dependent exon skipping was tested for its capability to regulate protein expression. The constructs M1–M5 were chosen for further analysis because they span the complete range from complete exon inclusion (M1) to nearly complete exon skipping (M5). The aim was to test them in the context of transgenes that allowed for quantification of the dynamic range at the protein level. As transgenes we chose a luciferase reporter gene and the transcription factor MAX (MYC-associated factor X). MAX is the central part of the MYC/MAX/MXD network of transcription factors that heterodimerizes with both MYC and its antagonists to regulate cell proliferation, differentiation and apoptosis (36).

An intron was inserted into the intron-less luciferase gene *luc*+ thereby dividing the luciferase open reading frame into two parts (intron 2 of the human β-globin gene *blg2* was used – *bgl2* intron). In a next step, exon 2 from the five selected minigene constructs M1-M5 along with 150 nucleotides of its flanking intron sequences was inserted into the middle of the *bgl2* intron. Using this approach, exons 1 and 3 comprised the coding sequence of *luc*+, whereas exon 2 originated from the minigene (Figure 3A). Skipping exon 2 would restore the coding sequence of the firefly luciferase. The incorporation of exon 2, however, would lead to a truncated, inactive firefly luciferase due to a premature stop codon located in exon 2. The selected exon-skipping devices of the minigene constructs M1 to M5 were transferred into the *bgl2* intron of the *luc*+ gene, which resulted in constructs L1 to L5, respectively. As controls, a construct harboring only exon 2 without the aptamer and a variant of L2 carrying a binding-deficient aptamer (L2-A13U) were created.

The same selection of constructs were cloned into the human MAX gene. The coding sequence was composed of the constitutive exons E1, E3, E4 and E5. The splicing devices (the tc aptamer-controlled exon 2 together with both flanking introns) were placed at the natural exon-exon-junction between exons 3 and 4 (Figure 3A) resulting in the constructs MAX1–MAX5. Similar to the luciferase constructs, exon skipping would restore the MAX reading frame, whereas exon inclusion introduces a premature stop codon. For protein detection, an N-terminal FLAG tag was added. The same controls as for luciferase (without aptamer and with binding-deficient aptamer) were created.

The switching capability of all devices (L1–L5 and MAX1–MAX5 and all respective controls) was analyzed both at the mRNA and at the protein level (Figure 3). Exon skipping was visualized by RT-PCR (Figure 3B) and quantified by RT-qPCR (Figure 3C). Protein levels were detected by luciferase assay and Western blot, respectively (Figure 3D). The observed data at the RNA level strongly resembled the results of the splicing analyses of the minigene constructs. Increasing P1 stability from L1 to L5 and MAX1 to MAX5, respectively, resulted in enhanced exon skipping in the absence of tc. The addition of tc further increased exon skipping for all constructs, with L5 and MAX5 showing only a low level of regulation due to nearly complete exon skipping in both the absence and presence of tc.

Detection of luciferase activity and the MAX protein levels by Western blot showed that the observed changes in the splicing patterns were transferred to protein expression.

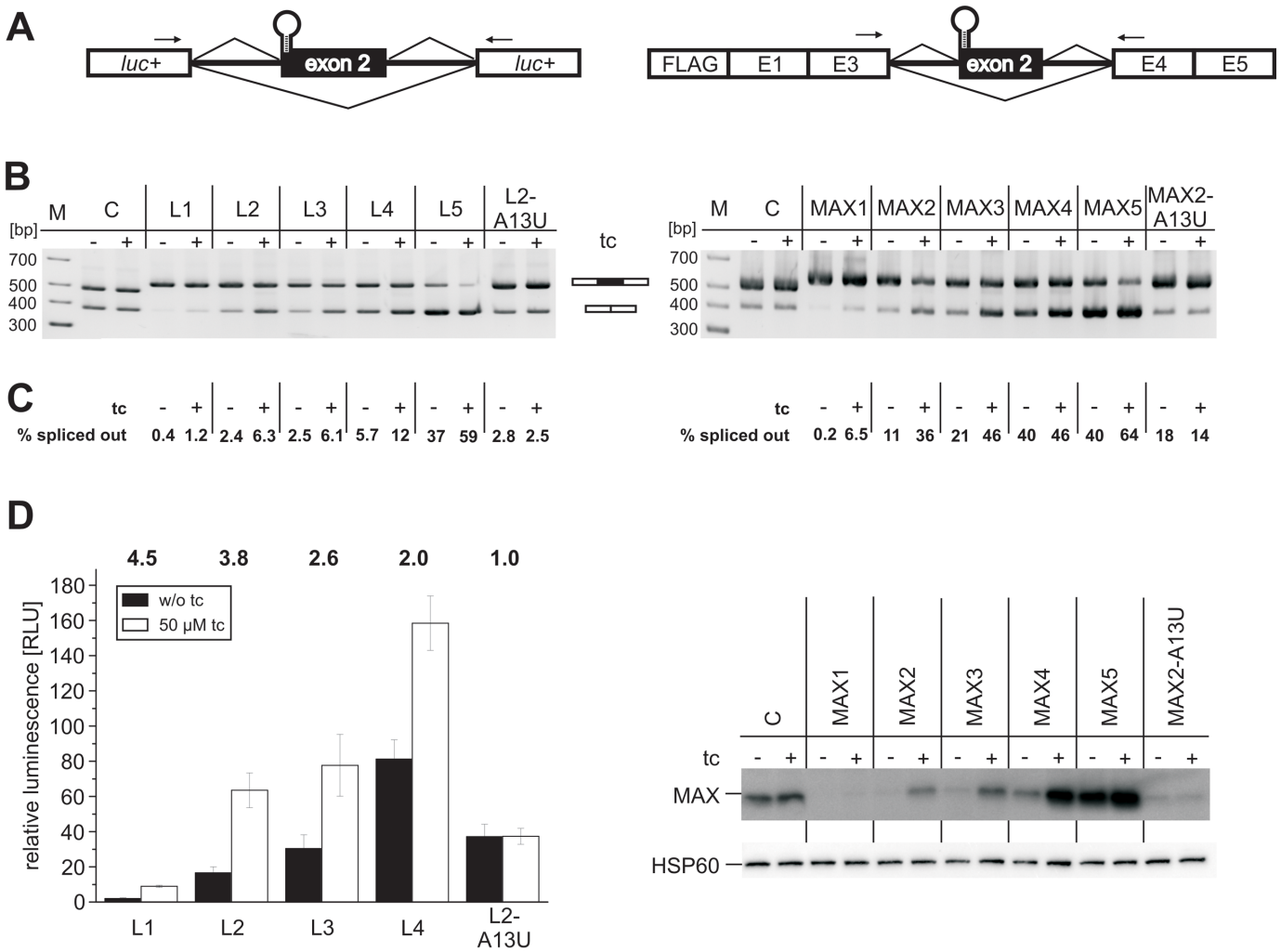

Figure 3. Regulation of a luciferase reporter gene and the transcription factor MAX. (**A**) Scheme of the splicing devices. Skipping exon E2 restored the open reading frame of the luciferase gene *luc*+ (left scheme). The aptamer-controlled exon E2 from the luciferase constructs was transferred into the coding region of the *MAX* gene between exon E3 and exon E4. A FLAG tag was located at the N-terminus of MAX for detection by western blot (right scheme). (**B**) HEK293 cells were transiently transfected with the constructs L1–L5 (left) and MAX1-MAX5 (right) and treated with or without 50 μM tc for 24 h. Total RNA was prepared and used for RT-PCR with primer pairs binding to both exons of *luc*+ and E3 and E4, respectively (indicted by arrows in A). C: control construct without the tc aptamer, M: Marker. L2/MAX2-A13U harbored a point mutation at position 13 of the aptamer. Due to this mutation, the aptamer is no longer able to bind tc. (**C**) RNA prepared as described in B was used for RT-qPCR for quantification. The percent of the exon spliced out is given. (**D**) Luciferase activity measurement of the respective constructs L1 to L5 and L2-A13U are shown on the left side. The ratios between the firefly and *Renilla* luciferase are shown. Numbers above the bars indicate the dynamic range of regulation for each construct. Error bars represent the standard deviation from the mean values. The value of the control construct without tc was set to 100. The protein expression of the constructs MAX1–5 was analyzed by Western blot analysis. Anti-FLAG was used to detect MAX fusion proteins, and anti-HSP60 was used as a loading control.

The activity increased from L1 to L5 and MAX1 to MAX5, respectively, in the absence of tc as did the amount of mRNA isoforms lacking exon 2. In the presence of tc, luciferase activity and MAX protein levels further increased, due to tc-dependent skipping of exon 2. Constructs 1 (L1 and MAX1) showed the highest regulation, with 4.5-fold increase upon tc addition for L1 and approximately 5-fold for MAX1 (gel quantified, Supplementary Figure S4), albeit with a low overall expression level. A slightly lower dynamic range of regulation was observed for construct 2 (L2 and MAX2), but with an expression level comparable to the control construct A13U. The construct which harbors a mutation in the tc binding pocket of the aptamer was used to verify that the observed regulation was due to the direct interaction of tc with the aptamer. As expected, the addition of tc had no impact on splicing patterns or luciferase activity of the construct with the binding-deficient aptamer, which again confirmed that the observed regulation was dependent on a functional device.

In sum, the data showed that the splicing device was able to control the expression of a mammalian gene, with splicing regulation directly translating into protein output and underscoring the genetic modularity and robustness of the device. Thus, the dynamic range of regulation found is in a similar range as many naturally occurring splicing events (37–39).

Robustness of the splicing riboswitch

We decided on construct 2 to further characterize the behavior of our regulatory device. It was chosen because it showed the best switching behavior at suitable protein levels.

Dose-dependency of the regulation was tested with increasing concentrations of tc ranging from 0 to 200 μM. In parallel, it was confirmed that tc was not toxic for the cells at the concentrations that were used. A cell viability assay showed no reduction in viability for up to 500 μM tc (Supplementary Figure S5). Figure 4A demonstrates that the luciferase activity of L2 increases with increasing concentration of tc. The values of the binding-deficient control construct L2-A13U only marginally increased, which may be attributed to residual binding but also to nonspecific stabilization of mRNA by tetracyclines (40). At 200 μM tc, the dynamic range of regulation increased up to 5.7-fold, which indicated that exon skipping can be efficiently controlled in a dose-dependent manner.

Furthermore, the impact of the promoter strength on the functionality of the device was analyzed. For this purpose, the strong CMV promoter of the L2 construct was exchanged for the weaker SV40 promoter. Figure 4B shows that an exchange of the promoter did not influence the switching behavior of the riboswitch. The functionality of the regulatory device was further compared in three additional cell lines, as alternative splicing is known to be highly cell-type specific. The L2 construct was compared in HEK293, HeLa, MCF-7 and A-549 cells. Figure 4C demonstrates that the regulatory device works in all of the tested cell lines. The expression in the OFF state is almost identical in HEK293 and in HeLa cells, while it is increased in MCF-7 and A-549 cells. In the ON state, the expression is similar in all four tested cell lines. A control construct containing no aptamer did only show marginal increase in fluorescence for both tested promoters and in either cell line probably due to nonspecific stabilization of the mRNA by tetracyclines. The data indicate that the riboswitch performance was cell-type independent. This benefit was probably conferred by the synthetic exon 2, which was composed of splicing-neutral sequences (31).

Taken together, construct 2 emerged as an efficient tc-dependent control element for exon skipping and represents a robust and dose-dependent switching device for controlling gene expression in mammalian cell lines.

Dual control of splicing and mRNA stability

Next, we tested if the newly developed splicing device L2 can be combined with other RNA-based regulators, such as a recently developed tc-controlled aptazyme (18). The aptazyme consists of the tc aptamer as a sensor fused to a hammerhead ribozyme used as an effector domain. Inserted into the 3′ untranslated region (UTR) of an mRNA, the aptazyme controls mRNA stability. In the absence of tc, the hammerhead was catalytically active and able to cleave off the polyA tail, which resulted in rapid mRNA degradation. The stabilization of the closing stem P1 of the aptamer domain by tc prevented an intramolecular loop-loop interaction within the hammerhead that was necessary for efficient catalysis *in vivo*. Consequently, and similar to our splicing device, the aptazyme allowed for induction of gene expression in the presence of tc (Figure 5A). A tc controlled aptazyme (named K19) with a dynamic range of 4.8-fold (18) was cloned into the 3′ UTR of the L2 construct. The resulting construct L2-K19 showed a significant reduced basal activity. The addition of tc increased luciferase activity by 7.3-fold (Figure 5B). Therefore, the combination of the two regulatory devices led to an additive effect with respect to the dynamic range of regulation.

Triggering cell death by the tc riboswitch controlled alternative splicing

The splicing device based on construct 2 turned out to be the most promising and valuable system. It was therefore chosen to explore the applicability of the device to control cellular decisions. We decided on a suicide gene to control cell death in a tc-dependent way. The CD20 protein is a surface receptor expressed on B cells. The treatment of CD20-expressing cells with the therapeutic antibody rituximab (RTX) efficiently mediated cell death via the combined action of several mechanisms, including the activation of apoptotic and inhibition of anti-apoptotic pathways, antibody-dependent cell-mediated cytotoxicity (ADCC) and complement-dependent cytotoxicity (CDC) (41). With this approach, RTX was used as a therapeutic modality to treat CD20 positive B cell malignancies (e.g. non-Hodgkin's lymphoma) (41,42).

The coding sequence of CD20 was divided in two parts by the insertion of the splicing device (tc aptamer-controlled exon 2 flanked with both introns from L2) into a natural exon-exon-junction. When exon 2 is skipped, the reading frame of CD20 is restored, allowing it to trigger apoptosis in the presence of RTX (Figure 6A). In the absence of tc, exon 2 is retained and CD20 is not expressed, consequently the cells survived in the presence of RTX. The device-equipped gene for CD20 was stably integrated into the HeLa cell line HF1–3 which did not express CD20 naturally using the Flp-In system (18,34). As a control, the coding sequence of CD20 without introns was integrated resulting in HF1–3CD20. RT-PCR analysis confirmed a tc-dependent exon skipping of the device also in the genetic context of the CD20 open reading frame (Figure 6B). Western blot analysis impressively demonstrates a marginal CD20 expression when tc was absent, but a significant increase in protein levels upon tc addition (Figure 6C).

A viability assay was performed to analyze the response of the cell line HF1–3C2 to RTX in the presence and absence of tc or the binding-incompetent derivative doxycycline (Figure 6D). The parental cell line HF1–3, which did not express CD20, served as a negative control and showed no response to RTX in the absence or presence of ligand. The cell line HF1–3CD20 however, which constitutively expresses CD20, did not survive the presence of RTX irrespective of the ligand tested. On the other hand, the cell line HF1–3C2 survived RTX treatment but was completely killed in the presence of tc. The prominent cell death in the presence of tc was comparable to the complete killing of cells that constitutively express CD20. Importantly, cells treated with doxycycline survived. Despite the fact that doxycycline differs from tc only by the position of one hydroxyl group, it is not bound by

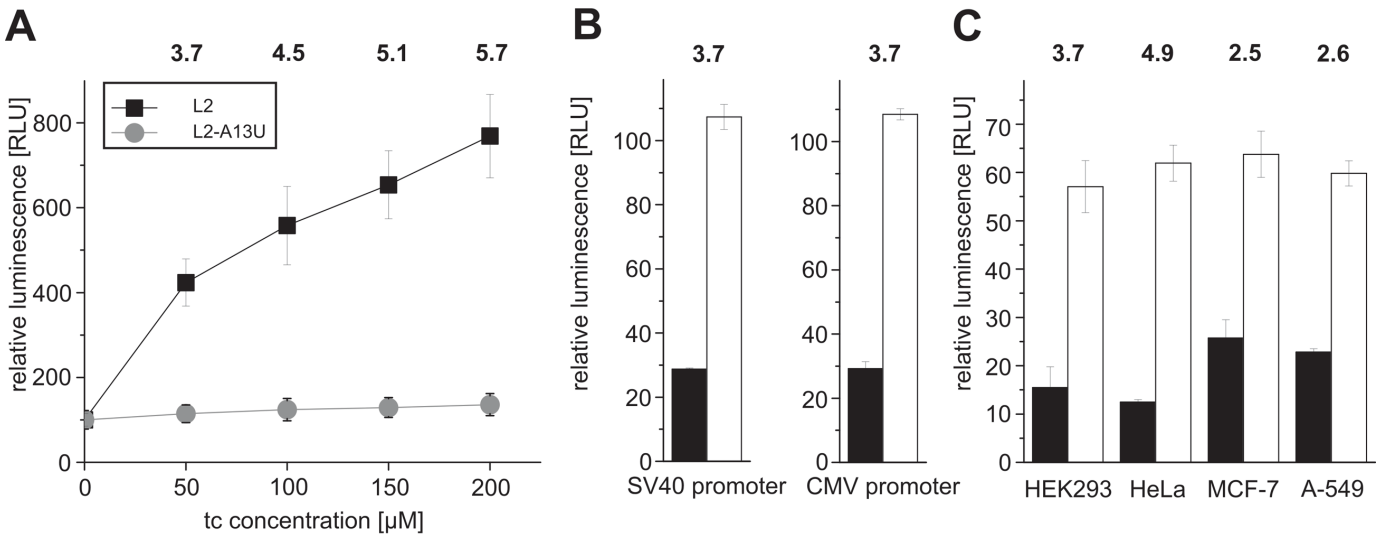

Figure 4. Robustness of the splicing riboswitch. (**A**) Dose-response curve of the luciferase construct L2 with increasing concentrations of tc. The binding-deficient construct L2-A13U was used as a control. The value of L2-A13U in the absence of tc was set to 100. (**B**) Luciferase assays of the construct L2 expressed from different promoters (**C**). Luciferase assays of construct L2 expressed in different cell lines. HEK293 cells (A, B) or different cell lines (C), as indicated, were transfected with the construct L2 and treated with or without 50 μM tc for 24 h. The ratios between the firefly and the *Renilla* luciferase are shown. The numbers above the bars indicate the dynamic range of regulation for each construct. Error bars represent the standard deviation from the mean values. The value of the control construct without tc was set to 100.

the tc aptamer (11). Survival of the cell line HF1–3C2 in the presence of doxycycline confirmed that the observed regulation was caused by the direct interaction of tc with its aptamer. Together, the data showed that the splicing device was capable of regulating cellular decisions in a chromosomal context.

DISCUSSION

Regulatory systems for the specific expression of transgenes are important and indispensable tools for research and synthetic biology application. Whereas the classical way is still the use of conditional promoters, they often suffer from limitations such as leaky basal expression, pleiotropic effects, species specificities (43,44) but also problems like metabolic burden or immunogenic responses caused by the heterologous expression of transcription factors. Moreover, a cell type specific expression is not possible. The use of RNA-based regulatory devices offers the advantage of being independent of heterologous protein expression. They provide the distinct advantage of modularity that allows for free combination of different sensor and actuator domains and offer the possibility to select sensor domains *de novo* (45). Moreover, synthetic riboswitches have been shown to be fully functional in yeast for all tested cases where leaky expression ruled out the use of the classical tet-on/off system (14). Beyond that, the combined control on different levels of gene expression allows for better fine-tuning of the required protein amount (46,47). It offers the chance to combine several regulatory devices that respond to the same or different input signals and allows for the construction of complex genetic circuits (48).

Many synthetic RNA devices have been developed for bacteria and yeast. However, the number of genetic devices to study cellular and molecular biology in mammalian cells is still very limited (49). This may be explained by the fact that there is very little transferability between microbes and higher eukaryotes (7). The mechanisms on which natural riboswitches in bacteria rely on, e.g. for transcriptional termination, are not applicable in eukaryotic cells due to the missing spatial and temporal coupling of transcription and translation. Beyond that, synthetic riboswitches developed in our lab that control translation initiation in yeast failed when tested in mammalian systems (7). Motivated by the extraordinary importance of splicing in mammalian cells, we attempted to develop a robust and modular synthetic riboswitch for conditional control of gene expression via the control of alternative splicing for the application in mammalian cells.

We exploited the tc aptamer, which is the most widely used sensor domain in RNA-based devices that respond to small molecules next to the theophylline aptamer. Tc binds to the aptamer with extremely high affinity and specificity and has a well characterized pharmacokinetic. Moreover, the aptamer has already successfully coupled to a variety of different actuator domains (12,15,18,50,51). An inherent feature of the tc aptamer is that ligand binding stabilizes the binding pocket and stabilization is also communicated to the adjacent closing stem P1 which otherwise undergoes significant breathing (13). Importantly, P1 is not involved in ligand binding and is therefore sequence-independent. This independence allowed the incorporation of functional sequences, which we exploited to control translation initiation in archaea (inclusion of the Shine-Dalgarno sequence into P1) (15) or intron retention in yeast (13). In the yeast system, the 5′ SS was inserted into the left arm of P1. Addition of tc inhibited recognition of the 5′ SS and lead to intron retention. 16-fold modulation of *gfp* expression was possible; however, the system was not transferrable to mammalian cells. Therefore, in the

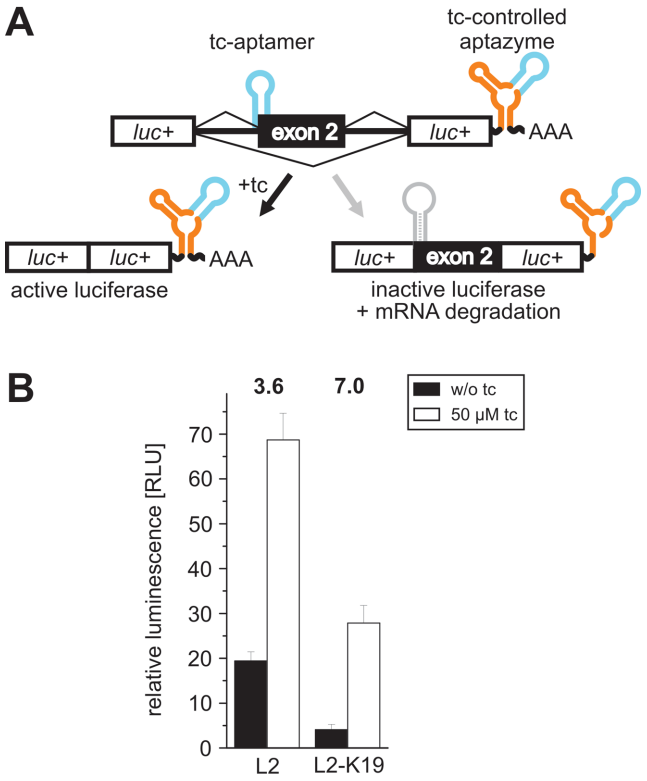

Figure 5. Dual control of splicing and mRNA stability. (**A**) Scheme of the dual control of luciferase expression by the tc aptamer (blue) of the developed splicing device and a tc-dependent aptazyme (hammerhead ribozyme with fused tc aptamer in orange and blue, respectively). In the absence of tc, the aptazyme was active and cleaved off the polyA tail. Therefore, the mRNA was degraded in the absence of tc. In the presence of tc, the aptazyme was inactive and exon 2 was skipped, so an active luciferase was produced. (**B**) Luciferase assay of the L2 construct and the aptazyme-containing construct L2-K19. C: control without tc aptamer/aptazyme. HEK293 cells were transfected with the constructs and treated with and without 50 μM tc for 24 h. The ratios between the firefly and the *Renilla* luciferase are shown. The numbers above the bars indicate the dynamic range of regulation for each construct. Error bars represent the standard deviation from the mean values. The value of the control without tc was set to 100.

current work we focused on the 3′ SS. The stability of P1 and consequently the degree of breathing allowed for fine-tuning expression levels starting from virtually no exon skipping observed for M1-based constructs with a lower stem stability to predominant exon skipping in M5-based constructs with high P1 stem stability. We varied stem length, stem stability and the relative location of the SS within P1 (Supplementary Table S2) and identified construct 2 (M2, L2, MAX2 and C2, respectively) as the best performing device with no or marginal skipping in the absence and a considerable amount of exon skipped when tc is present. This mRNA was then translated to a considerable amount that was sufficient to control cellular decisions, as shown by inducing cell death through tc-controlled CD20 expression. Exon skipping correlated with the stability and (Supplementary Table S2) but not with the overall stability of the aptamer (the exchange of P2 into a more stable stem-loop did not result in improved regulation, see M8 and M12). Based on our data a P1 stability <–

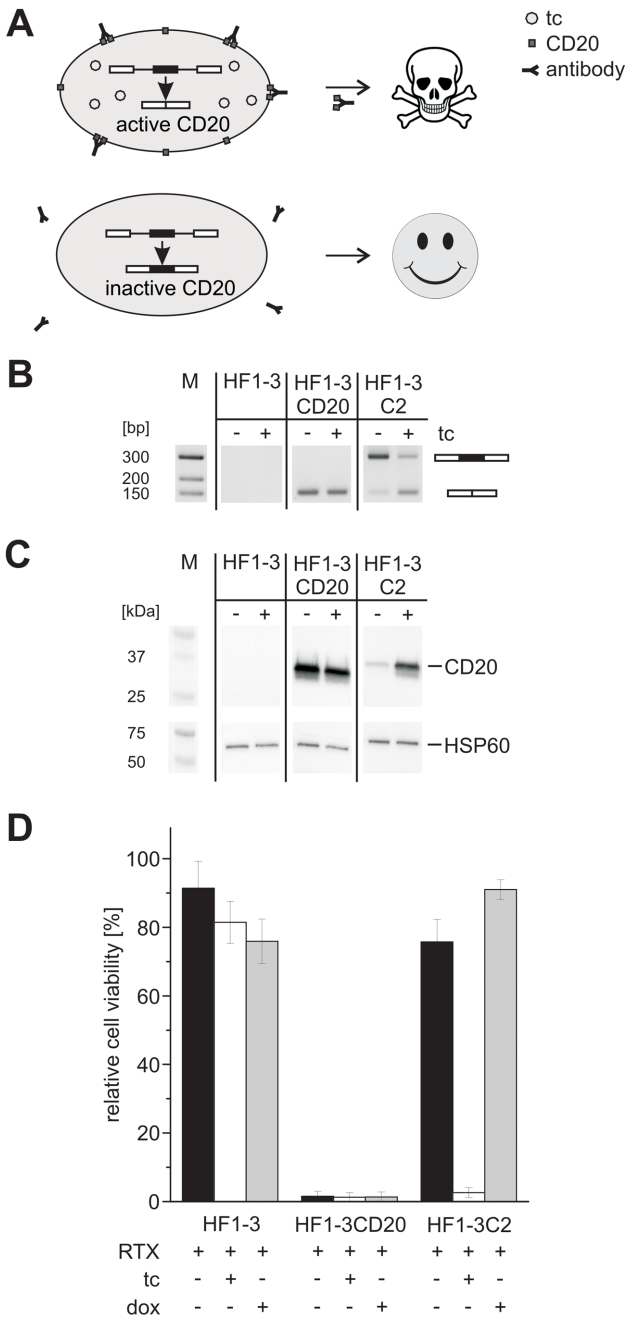

Figure 6. The tc aptamer controlled CD20 expression. (**A**) Schematic representation of the suicide system. When treated with the therapeutic antibody rituximab (RTX), cell death was induced in cells expressing CD20. As a positive control, CD20 was stably integrated into HeLa HF1–3 cells (cell line HF1–3CD20). The aptamer-controlled exon 2 along with the neighboring introns from construct L2 was inserted into the CD20 coding region, which resulted in the cell line HF1–3C2. In the presence of tc, exon 2 was skipped, the coding sequence of CD20 was restored, and apoptosis was triggered. Without tc, exon 2 was retained, which destroyed the CD20 reading frame and resulted in cell survival. (**B**, **C**) Cell lines were incubated with and without 50 μM tc for 2 days. Afterwards, RT-PCR and a western blot were performed. Primers used for RT-PCR bind to the coding sequence of CD20, which spans the alternatively spliced exon 2. HSP60 was used as a loading control for western blot. (**D**) Viability assay. The cell lines were incubated with and without RTX and 50 μM tc or doxycycline (dox) for 3 days. Afterwards, cell viability was analyzed by an AlamarBlue® assay. Error bars represent the standard deviation from mean values. For each cell line, the value of untreated cells was set to 100. The values of untreated cells are shown in Supplementary Figure S6.

24 kcal/mol favors exon skipping already in the absence of tc. Thus, a lower P1 stability, i.e. between –17 to –22 kcal/mol, performs best in our design strategy. However, further parameters, e.g. the location of the SS or the GC content, also influence the regulatory behavior.

The dynamic range of regulation obtained in our study was comparable with similar systems from the literature that also targeted control of exon skipping - not via a small molecule-controlled riboswitch but by proteins that bind their recognition sequence, thus interfering with splicing (24,25). Despite the apparently low dynamic range (2- to 4-fold), the observed regulation was sufficient to trigger cell death using an HSV-TK fusion protein (24). In the only study in which a small molecule binding aptamer was used, a 2-fold regulation was obtained using a minigene (23). Importantly, posttranscriptional events such as alternative splicing or other RNA-based mechanisms (e.g. miRNAs) are often found in this lower dynamic range, so we conclude that our newly developed splicing device follows the pattern observed in natural systems and therefore has the potential to be widely used for functional gene analyses (37–39).

In sum, here we present a robust, universally valid, portable and easily applicable device. Several inherent features reinforce these characteristics. We used a synthetic exon for the splicing device, which is supposed to be devoid of splicing enhancer and silencer sequences (31). The exon was specifically designed to encode no splicing regulatory sequences; hence its splicing efficiency is independent of the cell-type-specific expression of splicing factors and might also be resistant to cellular stresses impacting alternative splicing. Moreover, the use of a small, well-defined intron of the human β-globin gene as a host intron likely contributed to modularity. The *bgl2* intron is recognized in various heterologous contexts, enhances gene expression when added to intronless genes and has recently been exploited as a safety device for suicide gene therapy (52–56). A further strength of our splicing device is that the open reading frame of the targeted genes will not be changed. In this study, we showed functionality in four different contexts. Therefore, we anticipate that it will be transferable to additional genes, possibly any gene of interest. The device can be placed in the middle of any natural intron. The sequence identity of the portable device is given in Supplementary Figure S2 as underlined sequence. It consists of the aptamer-controlled exon 2 together with 150 nt of the flanking sequences on both sides. However, because natural introns can harbor splicing regulatory elements, different intron contexts might compromise device function. Alternatively, the exon together with the complete *bgl2* intron sequence (Supplementary Figure S2, black sequence) can completely be transferred into an open reading frame, as exemplified by the transfer of the device from luciferase to MAX or CD20. To facilitate recognition, it is favorable to place the device at a natural exon-exon junction. However, if such a junction is not available, the device can also be placed at any desired position, as shown with the firefly luciferase gene.

The splicing device can easily be combined with other regulatory systems. We demonstrated this by combination with a tc controlled aptazyme that impacted mRNA stability. Beyond that, the combinations with other aptazymes responding to ligands other than tc (50,57,58) would allow for graded responses to different input signals. Because promoter strength has no impact on performance, it should also be combinable with transcription factor-based devices. In addition, although alternative splicing is known to be highly cell type specific, the device was functional in four different cell lines demonstrating its robustness.

In conclusion, we developed a robust, genetic modular and portable device for the efficient control of alternative splicing in mammalian cells. Due to the design of the portable device, inclusion of the cassette exon leads to a non-functional protein. This limitation may be overcome by alternative design strategies in the future. However, for the splicing device developed here we predict that it will be widely employed for the regulation of other proteins but also RNA recognition sites that impact all levels of posttranscriptional gene regulation.

SUPPLEMENTARY DATA

Supplementary Data are available at NAR online.

ACKNOWLEDGEMENTS

We are grateful for the materials received from Prof. Dr. Lawrence Chasin (minigene) and Prof. Dr. Reinhard Lührmann (*bgl2* intron). Thank you also to Dr. Alexander Wittmann for his help and his support. Finally, we would like to thank Katharina Keim and Dr. Christian Berens for critical reading of the manuscript.

FUNDING

Deutsche Forschungsgemeinschaft [SFB902/A2 to B.S., SFB902/B14 to J.E.W.]; European Commission [H2020 ITN MetaRNA to B.S.]; LOEWE Schwerpunkt CompuGene. Funding for open access charge: LOEWE Schwerpunkt CompuGene.
Conflict of interest statement. None declared.

REFERENCES

1. Collins,J. (2012) Synthetic biology: bits and pieces come to life. *Nature*, **483**, S8–S10.
2. Qi,L.S. and Arkin,A.P. (2014) A versatile framework for microbial engineering using synthetic non-coding RNAs. *Nat. Rev. Microbiol.*, **12**, 341–354.
3. Roth,A. and Breaker,R.R. (2009) The structural and functional diversity of metabolite-binding riboswitches. *Annu. Rev. Biochem.*, **78**, 305–334.
4. Tuerk,C. and Gold,L. (1990) Systematic evolution of ligands by exponential enrichment: RNA ligands to bacteriophage T4 DNA polymerase. *Science*, **249**, 505–510.
5. Ellington,A.D. and Szostak,J.W. (1990) In vitro selection of RNA molecules that bind specific ligands. *Nature*, **346**, 818–822.
6. Berens,C. and Suess,B. (2015) Riboswitch engineering - making the all-important second and third steps. *Curr. Opin. Biotechnol.*, **31**, 10–15.
7. Berens,C., Groher,F. and Suess,B. (2015) RNA aptamers as genetic control devices: the potential of riboswitches as synthetic elements for regulating gene expression. *Biotechnol. J.*, **10**, 246–257.
8. Batey,R.T. (2015) Riboswitches: still a lot of undiscovered country. *RNA*, **21**, 560–563.
9. Wieland,M. and Hartig,J.S. (2008) Artificial riboswitches: synthetic mRNA-based regulators of gene expression. *Chem. Biol. Chem.*, **9**, 1873–1878.

10. Groher,F. and Suess,B. (2014) Synthetic riboswitches—a tool comes of age. *Biochim. Biophys. Acta.*, **1839**, 964–973.
11. Muller,M., Weigand,J.E., Weichenrieder,O. and Suess,B. (2006) Thermodynamic characterization of an engineered tetracycline-binding riboswitch. *Nucleic Acids Res.*, **34**, 2607–2617.
12. Suess,B., Hanson,S., Berens,C., Fink,B., Schroeder,R. and Hillen,W. (2003) Conditional gene expression by controlling translation with tetracycline-binding aptamers. *Nucleic Acids Res.*, **31**, 1853–1858.
13. Weigand,J.E. and Suess,B. (2007) Tetracycline aptamer-controlled regulation of pre-mRNA splicing in yeast. *Nucleic Acids Res.*, **35**, 4179–4185.
14. Kötter,P., Weigand,J.E., Meyer,B., Entian,K.D. and Suess,B. (2009) A fast and efficient translational control system for conditional expression of yeast genes. *Nucleic Acids Res.*, **37**, e120.
15. Demolli,S., Geist,M.M., Weigand,J.E., Matschiavelli,N., Suess,B. and Rother,M. (2014) Development of β-lactamase as a tool for monitoring conditional gene expression by a tetracycline-riboswitch in *Methanosarcina acetivorans*. *Archaea*, **2014**, 725610.
16. Ceres,P., Garst,A.D., Marcano-Velazquez,J.G. and Batey,R.T. (2013) Modularity of select riboswitch expression platforms enables facile engineering of novel genetic regulatory devices. *ACS Synth. Biol.*, **2**, 463–472.
17. Wittmann,A. and Suess,B. (2011) Selection of tetracycline inducible self-cleaving ribozymes as synthetic devices for gene regulation in yeast. *Mol. Biosyst.*, **7**, 2419–2427.
18. Beilstein,K., Wittmann,A., Grez,M. and Suess,B. (2015) Conditional control of mammalian gene expression by tetracycline-dependent hammerhead ribozymes. *ACS. Synth. Biol.*, **4**, 526–534.
19. Win,M.N. and Smolke,C.D. (2008) Higher-order cellular information processing with synthetic RNA devices. *Science*, **322**, 456–460.
20. Scotti,M.M. and Swanson,M.S. (2016) RNA mis-splicing in disease. *Nat. Rev. Genet.*, **17**, 19–32.
21. Wang,E.T., Sandberg,R., Luo,S., Khrebtukova,I., Zhang,L., Mayr,C., Kingsmore,S.F., Schroth,G.P. and Burge,C.B. (2008) Alternative isoform regulation in human tissue transcriptomes. *Nature*, **456**, 470–476.
22. Kim,D.S., Gusti,V., Pillai,S.G. and Gaur,R.K. (2005) An artificial riboswitch for controlling pre-mRNA splicing. *RNA*, **11**, 1667–1677.
23. Kim,D.S., Gusti,V., Dery,K.J. and Gaur,R.K. (2008) Ligand-induced sequestering of branchpoint sequence allows conditional control of splicing. *BMC Mol. Biol.*, **9**, 23.
24. Culler,S.J., Hoff,K.G. and Smolke,C.D. (2010) Reprogramming cellular behavior with RNA controllers responsive to endogenous proteins. *Science*, **330**, 1251–1255.
25. Hickey,S.F., Sridhar,M., Westermann,A.J., Qin,Q., Vijayendra,P., Liou,G. and Hammond,M.C. (2012) Transgene regulation in plants by alternative splicing of a suicide exon. *Nucleic Acids Res.*, **40**, 4701–4710.
26. Cooper,T.A. (2005) Use of minigene systems to dissect alternative splicing elements. *Methods*, **37**, 331–340.
27. Croft,M.T., Moulin,M., Webb,M.E. and Smith,A.G. (2007) Thiamine biosynthesis in algae is regulated by riboswitches. *Proc. Natl. Acad. Sci. U.S.A.*, **104**, 20770–20775.
28. Wachter,A., Tunc-Ozdemir,M., Grove,B.C., Green,P.J., Shintani,D.K. and Breaker,R.R. (2007) Riboswitch control of gene expression in plants by splicing and alternative 3' end processing of mRNAs. *Plant Cell*, **19**, 3437–3450.
29. Sudarsan,N., Barrick,J.E. and Breaker,R.R. (2003) Metabolite-binding RNA domains are present in the genes of eukaryotes. *RNA*, **9**, 644–647.
30. Bocobza,S., Adato,A., Mandel,T., Shapira,M., Nudler,E. and Aharoni,A. (2007) Riboswitch-dependent gene regulation and its evolution in the plant kingdom. *Genes Dev.*, **21**, 2874–2879.
31. Zhang,X.H., Arias,M.A., Ke,S. and Chasin,L.A. (2009) Splicing of designer exons reveals unexpected complexity in pre-mRNA splicing. *RNA*, **15**, 367–376.
32. Kemmerer,K. and Weigand,J.E. (2014) Hypoxia reduces MAX expression in endothelial cells by unproductive splicing. *FEBS Lett.*, **588**, 4784–4790.
33. Vogler,I., Newrzela,S., Hartmann,S., Schneider,N., von Laer,D., Koehl,U. and Grez,M. (2010) An improved bicistronic CD20/tCD34 vector for efficient purification and in vivo depletion of gene-modified T cells for adoptive immunotherapy. *Mol. Ther.*, **18**, 1330–1338.
34. Berens,C., Lochner,S., Lober,S., Usai,I., Schmidt,A., Drueppel,L., Hillen,W. and Gmeiner,P. (2006) Subtype selective tetracycline agonists and their application for a two-stage regulatory system. *ChemBioChem*, **7**, 1320–1324.
35. Al-Zoobi,L., Salti,S., Colavecchio,A., Jundi,M., Nadiri,A., Hassan,G.S., El-Gabalawy,H. and Mourad,W. (2014) Enhancement of Rituximab-induced cell death by the physical association of CD20 with CD40 molecules on the cell surface. *Int. Immunol.*, **26**, 451–465.
36. Diolaiti,D., McFerrin,L., Carroll,P.A. and Eisenman,R.N. (2015) Functional interactions among members of the MAX and MLX transcriptional network during oncogenesis. *Biochim. Biophys. Acta*, **1849**, 484–500.
37. Preussner,M., Goldammer,G., Neumann,A., Haltenhof,T., Rautenstrauch,P., Muller-McNicoll,M. and Heyd,F. (2017) Body Temperature Cycles Control Rhythmic Alternative Splicing in Mammals. *Mol. Cell*, **67**, 433–446.
38. Ip,J.Y., Tong,A., Pan,Q., Topp,J.D., Blencowe,B.J. and Lynch,K.W. (2007) Global analysis of alternative splicing during T-cell activation. *RNA*, **13**, 563–572.
39. Gueroussov,S., Gonatopoulos-Pournatzis,T., Irimia,M., Raj,B., Lin,Z.Y., Gingras,A.C. and Blencowe,B.J. (2015) An alternative splicing event amplifies evolutionary differences between vertebrates. *Science*, **349**, 868–873.
40. Wei,Y. and Bechhofer,D.H. (2002) Tetracycline induces stabilization of mRNA in Bacillus subtilis. *J. Bacteriol.*, **184**, 889–894.
41. Perez-Callejo,D., Gonzalez-Rincon,J., Sanchez,A., Provencio,M. and Sanchez-Beato,M. (2015) Action and resistance of monoclonal CD20 antibodies therapy in B-cell Non-Hodgkin Lymphomas. *Cancer. Treat. Rev.*, **41**, 680–689.
42. Cragg,M.S., Walshe,C.A., Ivanov,A.O. and Glennie,M.J. (2005) The biology of CD20 and its potential as a target for mAb therapy. *Curr. Dir. Autoimmun.*, **8**, 140–174.
43. Lienert,F., Lohmueller,J.J., Garg,A. and Silver,P.A. (2014) Synthetic biology in mammalian cells: next generation research tools and therapeutics. *Nat. Rev. Mol. Cell. Biol.*, **15**, 95–107.
44. Padidam,M. (2003) Chemically regulated gene expression in plants. *Curr. Opin. Plant. Biol.*, **6**, 169–177.
45. McKeague,M., Wong,R.S. and Smolke,C.D. (2016) Opportunities in the design and application of RNA for gene expression control. *Nucleic Acids Res.*, **44**, 2987–2999.
46. Deans,T.L., Cantor,C.R. and Collins,J.J. (2007) A tunable genetic switch based on RNAi and repressor proteins for regulating gene expression in mammalian cells. *Cell*, **130**, 363–372.
47. Garg,A., Lohmueller,J.J., Silver,P.A. and Armel,T.Z. (2012) Engineering synthetic TAL effectors with orthogonal target sites. *Nucleic Acids Res.*, **40**, 7584–7595.
48. Xie,Z., Wroblewska,L., Prochazka,L., Weiss,R. and Benenson,Y. (2011) Multi-input RNAi-based logic circuit for identification of specific cancer cells. *Science*, **333**, 1307–1311.
49. Mathur,M., Xiang,J.S. and Smolke,C.D. (2017) Mammalian synthetic biology for studying the cell. *J. Cell. Biol.*, **216**, 73–82.
50. Win,M.N. and Smolke,C.D. (2007) A modular and extensible RNA-based gene-regulatory platform for engineering cellular function. *Proc. Natl. Acad. Sci. U.S.A.*, **104**, 14283–14288.
51. Bayer,T.S. and Smolke,C.D. (2005) Programmable ligand-controlled riboregulators of eukaryotic gene expression. *Nat. Biotechnol.*, **23**, 337–343.
52. Chin,J.Y., Kuan,J.Y., Lonkar,P.S., Krause,D.S., Seidman,M.M., Peterson,K.R., Nielsen,P.E., Kole,R. and Glazer,P.M. (2008) Correction of a splice-site mutation in the beta-globin gene stimulated by triplex-forming peptide nucleic acids. *Proc. Natl. Acad. Sci. U.S.A.*, **105**, 13514–13519.
53. Kang,S.H., Cho,M.J. and Kole,R. (1998) Up-regulation of luciferase gene expression with antisense oligonucleotides: implications and applications in functional assay development. *Biochemistry*, **37**, 6235–6239.
54. Yuan,L., Janes,L., Beeler,D., Spokes,K.C., Smith,J., Li,D., Jaminet,S.C., Oettgen,P. and Aird,W.C. (2013) Role of RNA splicing in mediating lineage-specific expression of the von Willebrand factor gene in the endothelium. *Blood*, **121**, 4404–4412.
55. Haddad-Mashadrizeh,A., Zomorodipour,A., Izadpanah,M., Sam,M.R., Ataei,F., Sabouni,F. and Hosseini,S.J. (2009) A systematic study of the function of the human beta-globin introns on the

expression of the human coagulation factor IX in cultured Chinese hamster ovary cells. *J. Gene Med.*, **11**, 941–950.
56. Pourzadegan,F., Shariati,L., Taghizadeh,R., Khanahmad,H., Mohammadi,Z. and Tabatabaiefar,M.A. (2016) Using intron splicing trick for preferential gene expression in transduced cells: an approach for suicide gene therapy. *Cancer. Gene Ther.*, **23**, 7–12.
57. Klauser,B., Atanasov,J., Siewert,L.K. and Hartig,J.S. (2015) Ribozyme-based aminoglycoside switches of gene expression engineered by genetic selection in S. cerevisiae. *ACS Synth. Biol.*, **4**, 516–525.
58. Auslander,S., Ketzer,P. and Hartig,J.S. (2010) A ligand-dependent hammerhead ribozyme switch for controlling mammalian gene expression. *Mol. Biosyst.*, **6**, 807–814.
59. Xiao,H., Edwards,T.E. and Ferre-D'Amare,A.R. (2008) Structural basis for specific, high-affinity tetracycline binding by an in vitro evolved aptamer and artificial riboswitch. *Chem. Biol.*, **15**, 1125–1137.